

A Kinase Inhibitor Targeted to mTORC1 Drives Regression in Glioblastoma

Highlights

- The TORKi MLN0128 shows poor residence time, underlying poor *in vivo* efficacy
- RapaLink-1 shows improved potency compared with rapamycin and MLN0128
- RapaLink-1 binding to FKBP12 results in targeted and durable inhibition of mTORC1
- RapaLink-1 crosses the blood-brain barrier, blocking three brain cancer models *in vivo*

Authors

QiWen Fan, Ozlem Aksoy,
Robyn A. Wong, ..., Masanori Okaniwa,
Kevan M. Shokat, William A. Weiss

Correspondence

waweiss@gmail.com

In Brief

Fan et al. target mTORC1 activity in glioblastoma (GBM) with RapaLink-1, which is comprised of rapamycin linked to an mTOR kinase inhibitor. RapaLink-1 decreases mTORC1 activity in the brain and suppresses the growth of GBM xenografts and a genetically engineered mouse model of brain cancer *in vivo*.

A Kinase Inhibitor Targeted to mTORC1 Drives Regression in Glioblastoma

QiWen Fan,^{1,3} Ozlem Aksoy,^{1,3} Robyn A. Wong,^{1,3} Shirin Ilkhanizadeh,^{1,3} Chris J. Novotny,² William C. Gustafson,^{3,4} Albert Yi-Que Truong,^{4,5} Geraldine Cayanan,^{1,3} Erin F. Simonds,^{1,3} Daphne Haas-Kogan,⁶ Joanna J. Phillips,^{3,5} Theodore Nicolaides,^{4,5} Masanori Okaniwa,² Kevan M. Shokat,² and William A. Weiss^{1,3,4,5,*}

¹Department of Neurology

²Howard Hughes Medical Institute, Department of Cellular and Molecular Pharmacology
University of California, San Francisco, CA 94158, USA

³Helen Diller Family Comprehensive Cancer Center, San Francisco, CA 94158, USA

⁴Department of Pediatrics, University of California, San Francisco, CA 94158, USA

⁵Department of Neurological Surgery, University of California, San Francisco, CA 94158, USA

⁶Department of Radiation Oncology, Dana Farber Cancer Institute, Boston, MA 02215, USA

*Correspondence: waweiss@gmail.com

<http://dx.doi.org/10.1016/j.ccr.2017.01.014>

SUMMARY

Although signaling from phosphatidylinositol 3-kinase (PI3K) and AKT to mechanistic target of rapamycin (mTOR) is prominently dysregulated in high-grade gliial brain tumors, blockade of PI3K or AKT minimally affects downstream mTOR activity in glioma. Allosteric mTOR inhibitors, such as rapamycin, incompletely block mTORC1 compared with mTOR kinase inhibitors (TORKi). Here, we compared RapaLink-1, a TORKi linked to rapamycin, with earlier-generation mTOR inhibitors. Compared with rapamycin and Rapalink-1, TORKi showed poor durability. RapaLink-1 associated with FKBP12, an abundant mTOR-interacting protein, enabling accumulation of RapaLink-1. RapaLink-1 showed better efficacy than rapamycin or TORKi, potently blocking cancer-derived, activating mutants of mTOR. Our study re-establishes mTOR as a central target in glioma and traces the failure of existing drugs to incomplete/nondurable inhibition of mTORC1.

INTRODUCTION

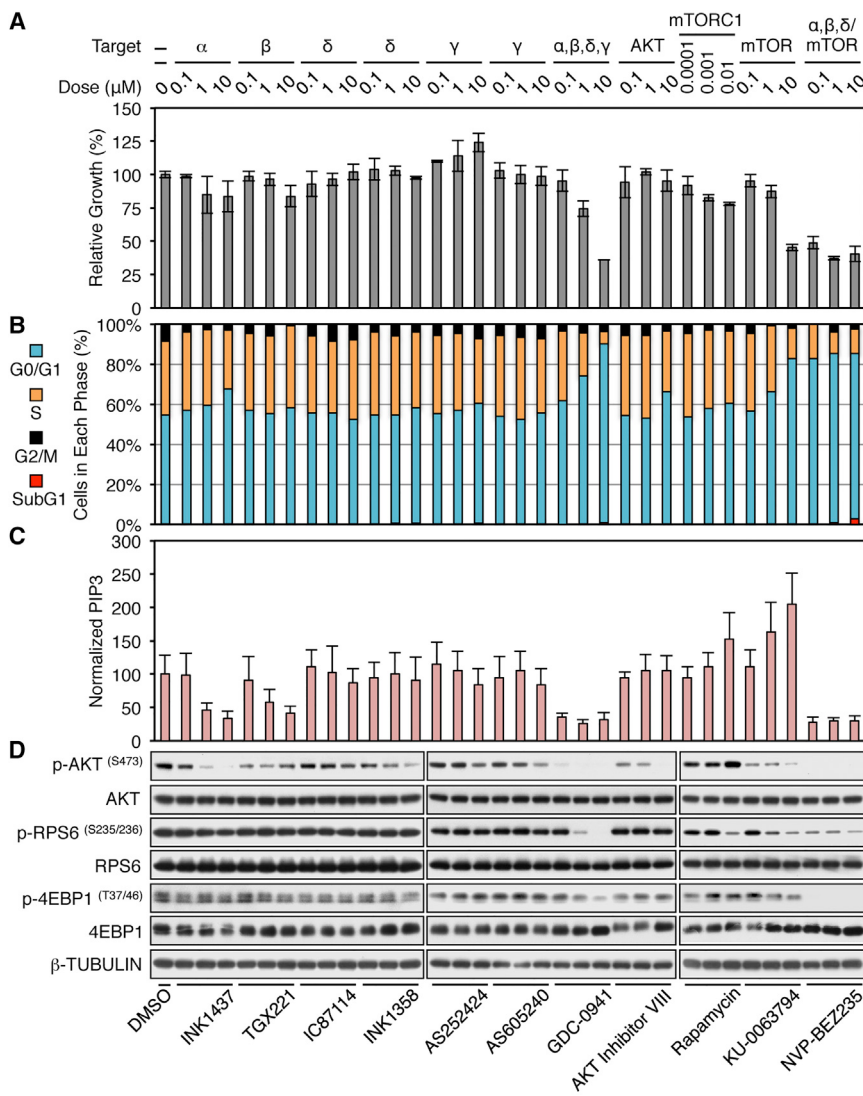
Glioblastoma (GBM), the most common primary brain tumor, represents one of the most aggressive cancers (Omuro and DeAngelis, 2013). Although signaling from phosphatidylinositol 3-kinase (PI3K) and AKT to mechanistic target of rapamycin (mTOR) is commonly dysregulated in GBM (Brennan et al., 2013), blockade of these upstream targets minimally affects mTOR activity in glioma (Fan et al., 2009). Direct targeting using allosteric inhibitors incompletely blocks mTORC1 activity (Feldman et al., 2009; Garcia-Martinez et al., 2009; Thoreen et al., 2009), while mTOR kinase inhibitors (TORKi) have not yet been fully evaluated in GBM.

mTOR exists in two distinct complexes, mTORC1 and mTORC2 (Loewith et al., 2002). With a half maximal inhibitory

concentration for mTORC1 inhibition in the high picomolar range, clinically approved first-generation mTOR inhibitors rapamycin and rapalogs sensitively and specifically inhibit mTORC1 through binding to the FK506 rapamycin binding (FRB) domain of mTOR with the aid of FK506 binding protein 12 (FKBP12) (Chiu et al., 1994; Loewith et al., 2002). Importantly, the FRB domain of mTOR is exposed in the mTORC1 but not the mTORC2 complex, which confers the mTORC1 specificity of rapalogs (Gaubitz et al., 2015). Second-generation TORKi act through orthosteric interactions with the ATP binding pocket of mTOR kinase (Feldman et al., 2009; Garcia-Martinez et al., 2009; Thoreen et al., 2009). As a result, TORKi blocks activation of substrates of mTORC1 and mTORC2, whereas rapalogs only impact mTORC1 (Feldman et al., 2009; Garcia-Martinez et al., 2009; Hsieh et al., 2012; Thoreen et al., 2009).

Significance

Glioblastoma (GBM), the most common primary brain tumor, numbers among the most aggressive of cancers. Dysregulated PI3K, AKT, and mTOR signaling is found in a majority of tumors; however, blockade of PI3K and AKT, which signal upstream of mTOR, fails to impact mTOR activity in GBM. We compared the first-generation allosteric mTOR inhibitor rapamycin and second-generation TORKi in vivo. Neither substantially impacted GBM. To improve upon earlier-generation inhibitors, we next tested a TORKi targeted specifically to mTORC1. RapaLink-1 drove regression of intracranial brain cancers in vivo, improving survival compared with earlier-generation inhibitors.



Recently developed mTORC1-directed inhibitors combine the high affinity of rapamycin for mTORC1 with the effective kinase inhibition of the TORKi MLN0128 (Rodrik-Outmezguine et al., 2016). The linker portion of this third-generation mTOR inhibitor lies in a channel in the mTORC1 complex, in a manner that does not disrupt linked rapamycin binding to FKBP12 or the FRB domain of mTOR. These inhibitors thus leverage the high selectivity and affinity of rapamycin for mTORC1 to specifically “deliver” MLN0128 to the ATP site of mTOR mainly in the mTORC1 complex.

RESULTS

mTOR Is a Central Therapeutic Target in GBM

To clarify the importance of mTOR as a target in GBM, we assessed proliferation (Figure 1A), cell cycle (Figure 1B), phosphatidylinositol 3,4,5-trisphosphate (PIP3) levels (Figure 1C), and activation of AKT, RPS6, and 4EBP1 (Figures 1D and S1) following treatment of LN229 cells with inhibitors targeting individual class I PI3Ks, a pan-inhibitor of class I PI3Ks, an inhibitor

Figure 1. mTOR Is an Attractive Therapeutic Target in GBM

(A) LN229 cells were treated for 3 days with inhibitors against PI3K (α , β , δ , or γ), pan-class I PI3K, AKT1/2, mTORC1, mTOR, and dual PI3K/mTOR inhibitors at the doses indicated. Proliferation was measured by WST-1 assay. Data shown represent mean \pm SD of triplicate measurements (percentage growth relative to DMSO-treated control).

(B) Flow cytometric analysis of cells treated as in (A) for 24 hr. Percentage of cells in G0/G1, S, and G2/M phases of cell cycle and apoptotic SubG1 fractions are indicated. Data shown represent mean \pm SD of triplicate measurements.

(C) Cells were treated as in (A) for 3 hr. Lipids were extracted and analyzed by ELISA. Data shown represent mean \pm SD of triplicate measurements. Samples were normalized to DMSO treatment.

(D) Western blotting analysis of cells from (B). Cells were harvested, lysed, and analyzed as indicated. Cell lysates were from a single experiment. Gels were run for the same period of time, and blots were processed with equivalent exposure times, to assure reproducibility. Representative blots from two independent experiments are shown. The names of the inhibitors against the targets shown in (A) are indicated below the blots. See also Figure S1.

of AKT, an inhibitor of mTORC1, a TORKi, and a dual inhibitor of PI3K and mTOR. Decreased proliferation (Figure 1A) and arrest in G0/G1 (Figure 1B) correlated with blockade of mTORC1, as assessed by decreased p-RPS6^{S235/236} and p-4EBP1^{T37/46} (Figures 1D and S1). No correlation to proliferation was evident with the abundance of PIP3 or mTORC2 inhibition, as assessed by p-AKT^{S473} (Figures 1C and 1D). Only the abundance of the mTOR target p-4EBP1^{T37/46} correlated consistently and directly with proliferation in GBM cells (Figures 1A, 1D, and S1).

An inhibitor of PI3K α induced modest blockade of proliferation and G1 arrest, while an inhibitor of PI3K β induced modest proliferative blockade without G1 arrest. Agents that blocked other class I PI3Ks reduced levels of the PIP3, but failed to affect proliferation or arrest at G1 (Figures 1A–C). The allosteric mTOR inhibitor rapamycin reduced p-RPS6^{S235/236} but not p-4EBP1^{T37/46}, led to increased levels of PIP3 and p-AKT^{S473}, and minimally affected proliferation. In contrast, the TORKi KU-0063794 (Garcia-Martinez et al., 2009) showed dose-dependent reduction of p-RPS6^{S235/236}, p-4EBP1^{T37/46}, and p-AKT^{S473}, with a corresponding blockade of proliferation. Similar to rapamycin, KU-0063794 increased levels of PIP3, in accordance with a well-established mTORC1-negative feedback loop leading to reactivation of PI3K signaling (Sun et al., 2005). The pan-class I PI3K inhibitor GDC-0941 (Folkes et al., 2008) and the PI3K/mTOR inhibitor BEZ235 elicited cellular effects solely at doses sufficient to block mTOR directly (Figures 1A–D). Data in Figures 1 and S1 suggest that blockade of mTORC1 was critical, whereas blockade

of mTORC2 was dispensable for the anti-proliferative activity of PI3K and mTOR inhibitors in GBM, and reaffirm the importance of the mTORC1 target p-4EBP1^{T37/46} as a robust biomarker.

Rapalink-1 Is More Potent than First- and Second-Generation mTOR Inhibitors

We next tested RapaLink-1 and RapaLink-2, two different third-generation mTOR inhibitors that link MLN0128 to rapamycin but differ in linker lengths (Figure S2A). RapaLink-1 more potently reduced levels of both p-4EBP1 and proliferation, as compared with RapaLink-2 (Figures 2A, 2B, S2B, and S2C). We compared rapamycin, RapaLink-1, and MLN0128 in LN229 and U87MG. Both growth inhibition and arrest in G0/G1 were more potent in response to RapaLink-1, compared with rapamycin or MLN0128 (Figures 2B and S2D). Rapamycin only inhibited the mTORC1 target p-RPS6^{S235/236} (Figures 2A and S2E). MLN0128, in contrast, inhibited the mTORC1 targets p-RPS6^{S235/236} and p-4EBP1^{T37/46}, as well as mTORC2 targets p-AKT^{S473}, p-SGK1^{S78}, and p-NDRG1^{T346}, and the p-AKT^{S473} target p-GSK3 β ^{S9} in a dose-dependent manner. RapaLink-1 selectively inhibited p-RPS6^{S235/236} and p-4EBP1^{T37/46} at doses as low as 1.56 nM. The mTORC2 targets p-AKT^{S473}, p-SGK1^{S78}, and p-NDRG1^{T346}, and the p-AKT^{S473} target p-GSK3 β ^{S9} was inhibited only at high doses, without further affecting growth (Figures 2A and 2B). Results were similar in two human GBM cell lines, LN229 and U87MG, lines ectopically expressing epidermal growth factor receptor (EGFR) and the GBM-derived variant EGFRvIII (Taylor et al., 2012), and in short-term cultures of GBM43, GBM5, and GBM12 from patient-derived xenografts (Figures S2F–S2L) (Sarkaria et al., 2006).

GBMs may develop new drivers in response to therapy, including activating mutations in mTOR itself. We therefore investigated RapaLink-1 in GBM cells engineered to express wild-type or tumor-derived mTOR, activating mTOR mutants: mTOR^{R2505P} and mTOR^{S2115Y} (Sato et al., 2010). RapaLink-1 potently decreased proliferation of cells expressing either wild-type or mutationally activated mTOR (Figure 2C), whereas cells expressing mutant mTOR showed reduced sensitivity to MLN0128. Although rapamycin treatment resulted in a substantial and similar effect on growth regardless of mTOR status, this was less potent than the effect observed with RapaLink-1. RapaLink-1 blocked p-4EBP1^{T37/46} irrespective of mTOR mutational status (Figure 2D). In contrast, levels of p-4EBP1^{T37/46} persisted in mTOR mutant lines treated with rapamycin and MLN0128. These results demonstrate that RapaLink-1 is more potent than first- and second-generation mTOR inhibitors.

MLN0128 blocks the mTORC2 targets p-AKT^{S473}, p-SGK1^{S78}, and p-NDRG1^{T346} at doses that also block mTORC1 targets, whereas RapaLink-1 shows modest selectivity for mTORC1 over mTORC2 (Figures 2A, S2E, S2F, S2H, S2J, and S2L). To further address the importance of mTORC2 inhibition, we combined inhibitors of mTOR with an inhibitor of AKT. Addition of the pleckstrin-homology domain inhibitor MK-2206 (Hirai et al., 2010) did not enhance the efficacy of MLN0128 or RapaLink-1, while it modestly enhanced the activity of rapamycin (Figure S2M). None of the mTOR inhibitors alone or in combination with MK-2206 had cytotoxic effects (Figure S2N). These results suggest that additional blockade of mTORC2 does not substantially improve the efficacy of mTORC1 inhibitors.

RapaLink-1 Shows Potent Anti-tumor Efficacy In Vivo

Prior to evaluating efficacy in vivo, we first evaluated toxicity, demonstrated by changes in weight (Figure S3A) and effects on blood counts and serum chemistries (Figure S3B). BALB/C^{nu/nu} mice bearing U87MG intracranial xenografts were treated with daily intraperitoneal (i.p.) injections of vehicle, MLN0128, or rapamycin or treated every 5 days with RapaLink-1. Mice did not gain or lose weight on RapaLink-1 when dosed every 5 days, but mice did gain weight when dosed every 7 days (Figure S3A). We next treated mice with daily i.p. injections of vehicle, MLN0128 and rapamycin; or RapaLink-1 given on days 1 and 6. Serum chemistries and complete blood counts, measured on days 1, 3, and 7, did not differ among treated or control groups (Figure S3B). Thus, we observed no significant toxicities associated with RapaLink-1 treatment.

To evaluate penetration across the blood-brain barrier, we treated normal BALB/C^{nu/nu} mice with rapamycin, MLN0128, and RapaLink-1 and examined the acute effects of these drugs on insulin signaling in skeletal muscle, liver, and brain tissues (Figure 3A). RapaLink-1 was able to inhibit p-RPS6^{S235/236} and p-4EBP1^{T37/46} in a dose-dependent manner in brain, but it did not inhibit the mTORC2 substrate p-AKT^{S473} in vivo (Figure 3A).

Having confirmed that RapaLink-1 inhibits mTORC1 activity in the brain, we next established intracranial xenografts, and the mice were treated with daily i.p. injections of MLN0128 or rapamycin or every 5 or 7 days with RapaLink-1. We assessed tumor burden (Figures 3B and 3C), mTOR signaling (Figure 3D), and survival (Figure 3E). RapaLink-1 led to initial regression and subsequent stabilization of tumor size, while tumors treated with vehicle, rapamycin, or MLN0128 grew steadily (Figures 3B and 3C). Western blotting analysis of treated tumors demonstrated that RapaLink-1 efficiently blocked p-4EBP1^{T37/46}, whereas MLN0128 and rapamycin only modestly blocked p-4EBP1^{T37/46} (Figure 3D). All treatments blocked p-RPS6^{S235/236}, while MLN0128 uniquely inhibited p-AKT^{S473}. We followed mice on therapy for 14 weeks. RapaLink-1 was well tolerated and associated with significantly improved survival ($p = 0.0238$, vehicle versus MLN0128; $p = 0.0011$, vehicle versus rapamycin; $p < 0.0001$, vehicle versus RapaLink-1, log rank analysis; $n = 9$ mice per group) (Figure 3E). Treated tumors showed decreased proliferation in response to RapaLink-1 but were only modestly affected by earlier-generation inhibitors of mTOR (Figures 3F and 3G).

To extend these data, we next compared RapaLink-1, MLN0128, and rapamycin in a patient-derived GBM xenograft, GBM43 (Sarkaria et al., 2006), again assaying tumor burden and survival. Since rapamycin showed some efficacy in vivo dosed at 1.5 mg/kg (Figure 3), we increased the dose to 5 mg/kg, close to the maximum tolerated dose (Houghton et al., 2010). We again established intracranial xenografts and treated with daily i.p. injections of MLN0128 or rapamycin or every 5 days with RapaLink-1. Tumors treated with RapaLink-1 showed decreased tumor growth as assessed by luciferase signal compared with tumors treated with vehicle, rapamycin, or MLN0128 (Figures 4A and 4B). Western blotting of treated tumor isolates demonstrated that RapaLink-1 efficiently blocked p-4EBP1^{T37/46}, whereas both MLN0128 and rapamycin only modestly blocked p-4EBP1^{T37/46}. All treatments blocked p-RPS6^{S235/236}, and MLN0128 again uniquely inhibited

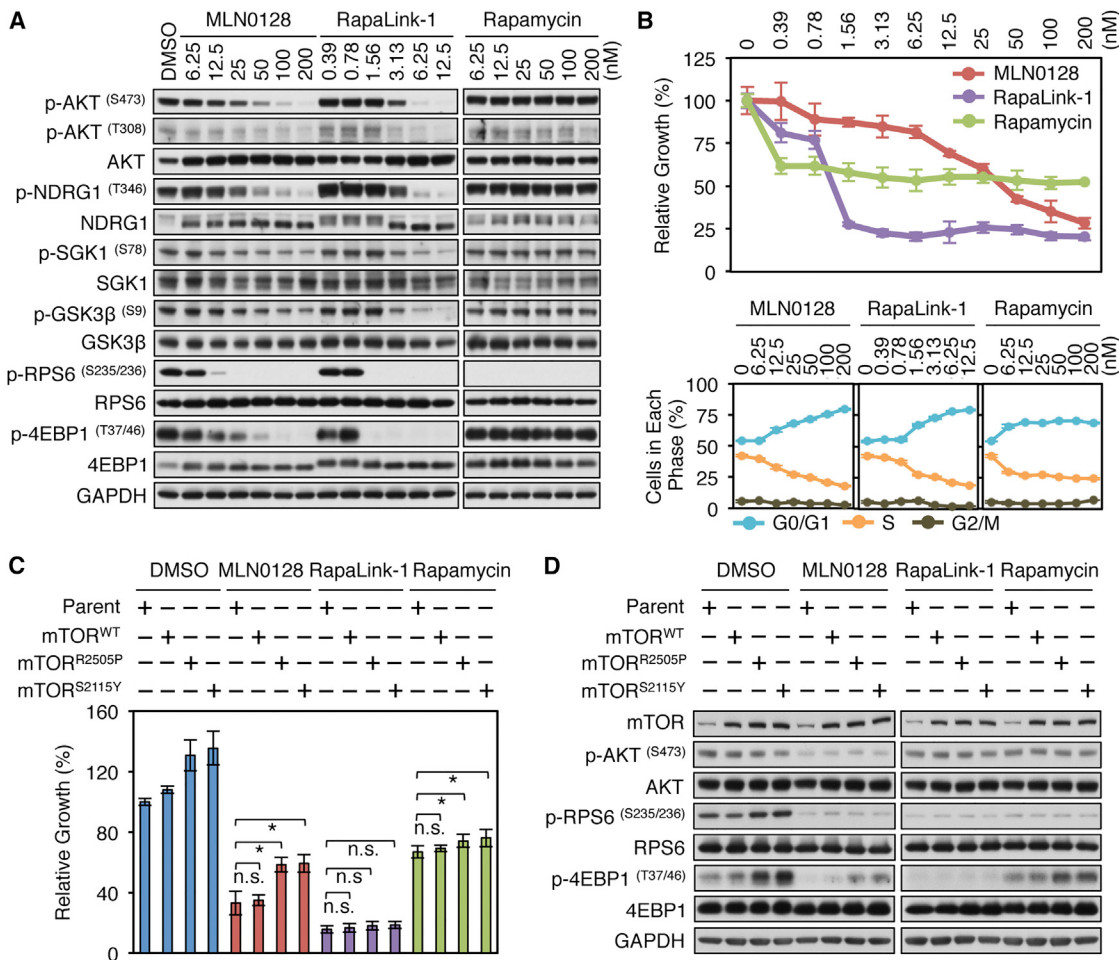


Figure 2. RapaLink-1 Is More Potent than First- and Second-Generation mTOR Inhibitors

(A) U87MG cells were treated with MLN0128, RapaLink-1, or rapamycin at the doses indicated for 3 hr, and harvested, lysed, and analyzed by western blotting as indicated. Cell lysates were from a single experiment. Gels were run for the same period of time, and blots were processed with equivalent exposure times, to assure reproducibility. Representative blots from three independent experiments are shown.

(B) Proliferation of U87MG cells treated as indicated for 3 days was measured by WST-1 assay (top panel). $p = 0.1621$, RapaLink-1 (1.5 nM) versus RapaLink-1 (3.13 nM); $p = 0.0792$, RapaLink-1 (1.56 nM) versus RapaLink-1 (6.25 nM); $p = 0.2169$, RapaLink-1 (1.56 nM) versus RapaLink-1 (12.5 nM); two-tailed Student's *t* test. Data shown represent mean \pm SD of triplicate measurements (percentage growth relative to DMSO-treated control). Flow cytometric analysis of U87MG cells treated as indicated for 24 hr (bottom panels). The percentage of cells in G0/G1, S, and G2/M phases is indicated. Data shown represent mean \pm SD of triplicate measurements.

(C) LN229 cells transfected stably with mTOR^{WT}, mTOR^{R2505P}, or mTOR^{S2115Y} were treated with 200 nM MLN0128, 1.56 nM RapaLink-1, or 10 nM rapamycin for 3 days. Proliferation was measured by WST-1 assay. Data shown represent mean \pm SD of triplicate measurements (percentage growth relative to DMSO-treated control). n.s., not significant; * $p < 0.05$ by two-tailed Student's *t* test.

(D) Cells treated as in (C) for 3 hr were harvested, lysed, and analyzed by western blotting as indicated. Cell lysates were from a single experiment. Gels were run for the same period of time, and blots were processed with equivalent exposure times, to assure reproducibility. Representative blots from two independent experiments are shown. See also Figure S2.

p-AKT^{S473} (Figure 4C). We followed mice on therapy for 43 days. RapaLink-1 was well tolerated and associated with significantly improved survival ($p = 0.0120$, vehicle versus MLN0128; $p = 0.0015$, vehicle versus rapamycin; $p = 0.0002$, vehicle versus RapaLink-1; log rank analysis; $n = 7$ mice per group) (Figures 4D and 4E). Treated tumors showed decreased proliferation in response to RapaLink-1, and again were only modestly affected by earlier-generation inhibitors of mTOR (Figures 4F and 4G). Because intracranial injection of GBM cells may disrupt the blood-brain barrier, we also tested the effects of RapaLink-1 on tumor burden in a genetically engineered "GTML" model in

which medulloblastoma tumors arise spontaneously without mechanical disruption of the barrier and in which luciferase is driven as a transgene (Swartling et al., 2010). GTML mice were treated by i.p. injections of vehicle or RapaLink-1 (1.5 mg/kg, every 5 days). RapaLink-1 again showed clear anti-tumor efficacy in these barrier-intact mice, blocking both p-RPS6^{S235/236} and p-4EBP1^{T37/46} (Figures 4H–4J).

RapaLink-1 Durably Blocks mTORC1

FKBP12 is an abundant cellular protein (MacMillan, 2013), and it is expressed at high levels in human GBMs (Figure S4A). The

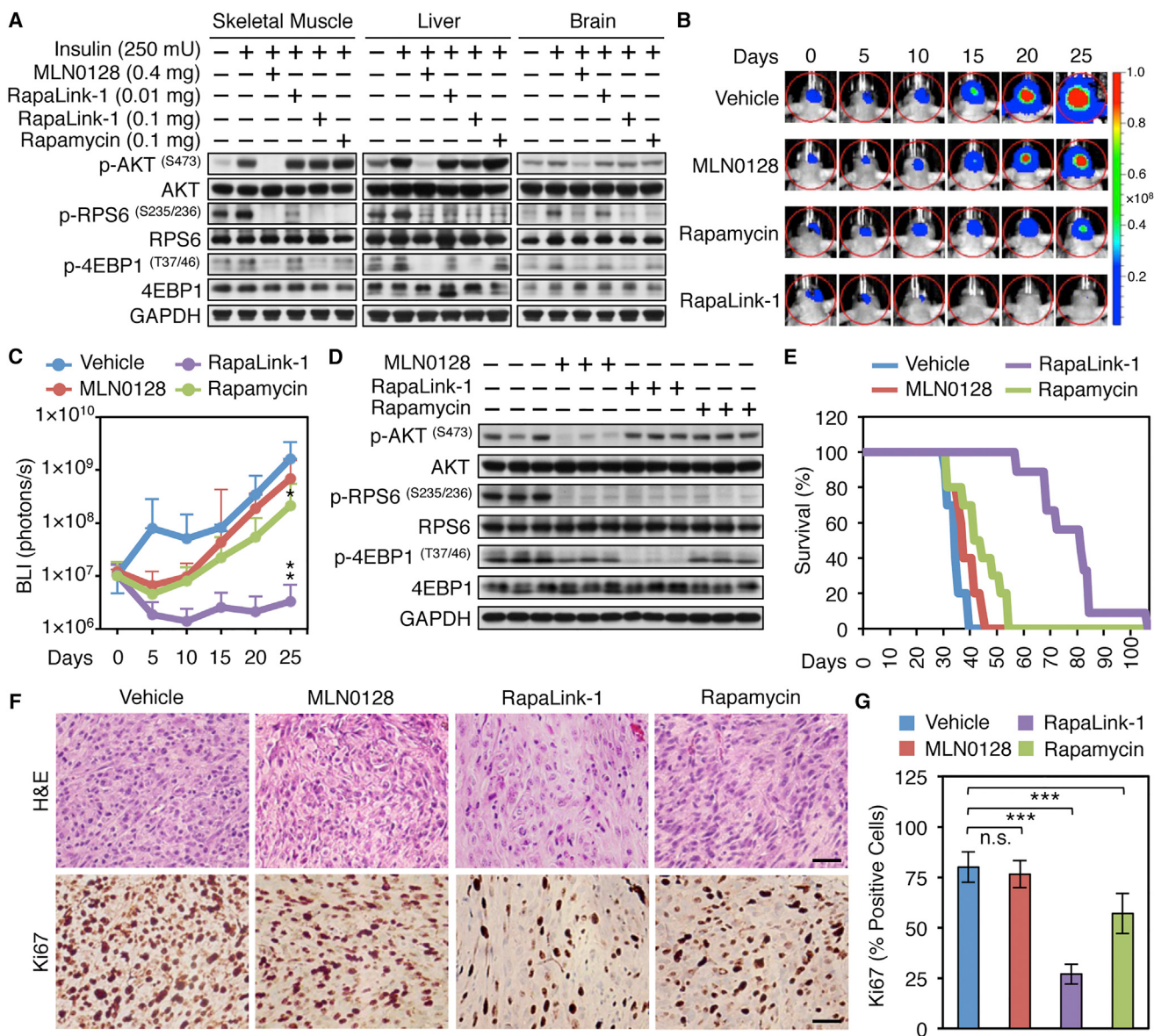


Figure 3. Comparative Efficacy of MLN0128, RapaLink-1, and Rapamycin in Orthotopic GBM Xenografts

(A) BALB/c^{nu/nu} mice were treated with i.p. injections of vehicle, MLN0128 (16 mg/kg), RapaLink-1 (0.4 or 4 mg/kg) or rapamycin (1.5 mg/kg) for 15 min, followed by i.p. injection of 250 mU insulin or saline for 15 min. Mice were euthanized, and skeletal muscle, liver, and brain were harvested, lysed, and analyzed by western blotting as indicated.

(B) U87MG cells expressing firefly luciferase were injected intracranially into BALB/c^{nu/nu} mice. After tumor establishment, mice were sorted into four groups and treated by i.p. injections of vehicle (daily), MLN0128 (1.5 mg/kg, daily), RapaLink-1 (1.5 mg/kg, every 5 or 7 days), or rapamycin (1.5 mg/kg, daily). Bioluminescence imaging of tumor-bearing mice was obtained at days shown (day 0 was start of treatment), using identical imaging conditions.

(C) Dynamic measurements of bioluminescence intensity (BLI) in treated tumors over time. Regions of interest from displayed images were revealed on the tumor sites and quantified as maximum photons/s/cm² squared/steradian. Data shown represent mean of photon flux ± SD from n = 12 mice. *p < 0.05, vehicle versus rapamycin; **p < 0.01, vehicle versus RapaLink-1; n.s., not significant, vehicle versus MLN0128 (two-tailed Student's t test on day 25).

(D) Animals were euthanized when showing signs of illness, per IACUC protocol. Thirty min prior to being euthanized, three animals from each group treated as in (B) were injected with vehicle, MLN0128 (1.5 mg/kg), RapaLink-1 (1.5 mg/kg), or rapamycin (1.5 mg/kg). Tumors were harvested, lysed, and analyzed by western blotting as indicated.

(E) Survival curves of BALB/c^{nu/nu} mice injected intracranially with U87MG cells. Five days after tumor implantation, mice were treated by i.p. injection of vehicle (daily), MLN0128 (1.5 mg/kg, daily) for 46 days, RapaLink-1 (1.5 mg/kg, every 5 days for 25 days, then once a week for 11 weeks), or rapamycin (1.5 mg/kg, daily). p = 0.0238, vehicle versus MLN0128; p = 0.0011, vehicle versus rapamycin; p < 0.0001, vehicle versus RapaLink-1, log rank analysis; n = 9 mice per group.

(F) Three animals from each group were euthanized on day 25. Samples were stained with H&E, and proliferating tumor cells were identified by immunohistochemistry for Ki67. Panel shows representative images. Scale bars, 100 μm.

(G) Data shown represent mean ± SD of five high-power microscopic fields from each of three tumors in each group. n.s., not significant; ***p < 0.001 by two-tailed Student's t test. See also Figure S3.

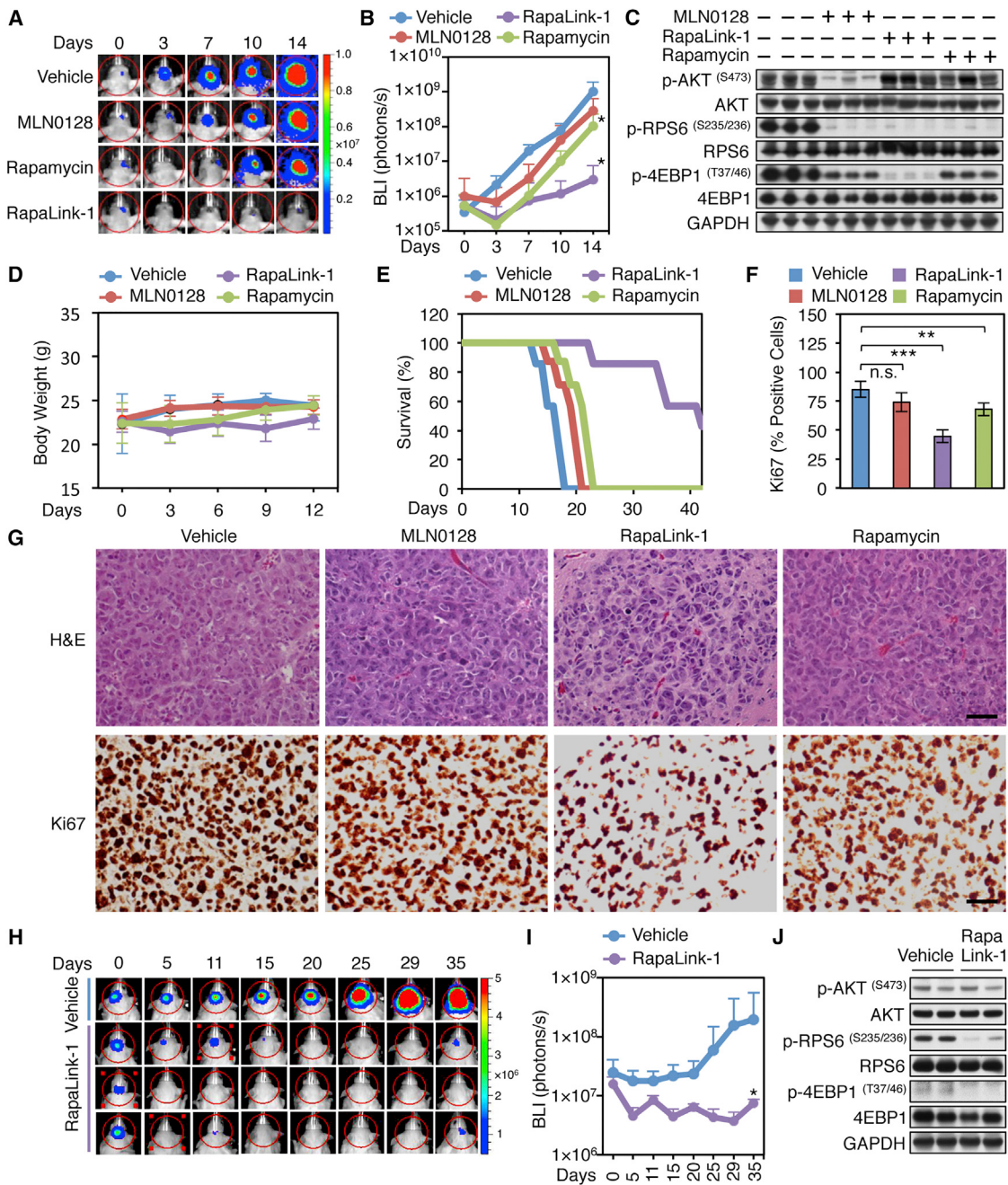


Figure 4. Comparative Efficacy of MLN0128, RapaLink-1, and Rapamycin in an Orthotopic Patient-Derived Xenograft and Genetically Engineered Models

(A) GBM43 cells (1×10^5) expressing firefly luciferase were injected intracranially in BALB/c^{nu/nu} mice. After tumor establishment, mice were sorted into groups, and treated by i.p. injections of vehicle (daily), MLN0128 (1.5 mg/kg, daily), RapaLink-1 (1.5 mg/kg, every 5 days), or rapamycin (5 mg/kg, daily). Bioluminescence imaging of tumor-bearing mice was obtained at days 0, 3, 7, 10, and 14 (after starting treatment) using identical imaging conditions.

(B) Dynamic measurements of bioluminescence intensity (BLI) in treated tumors from (A). Regions of interest from displayed images were revealed on the tumor sites and quantified as maximum photons/s/cm²/steradian. Data shown are mean \pm SD of n = 10 mice in each group. p = 0.0801, vehicle versus MLN0128; *p = 0.0254, vehicle versus rapamycin; *p = 0.0145, vehicle versus RapaLink-1 (two-tailed Student's t test on day 14).

(C) Animals were euthanized when showing signs of illness, as per IACUC protocol. Three animals from each group treated as in (A) (daily for rapamycin and MLN0128, and every 5 days for RapaLink-1) were injected with vehicle, MLN0128 (1.5 mg/kg), RapaLink-1 (1.5 mg/kg), or rapamycin (5 mg/kg) 30 min prior to being euthanized. Tumors were harvested, lysed, and analyzed by western blotting as indicated.

(D) Body weights of mice in (A) were measured every 3 days for 12 days. Data shown are mean \pm SD from n = 10 mice in each group.

(E) Survival curves of BALB/c^{nu/nu} mice injected intracranially with GBM43 cells. Three days after tumor implantation, mice were treated by i.p. injection of vehicle (daily), MLN0128 (1.5 mg/kg, daily), RapaLink-1 (1.5 mg/kg, every 5 days), or rapamycin (5 mg/kg, daily). p = 0.0120, vehicle versus MLN0128; p = 0.0015, vehicle versus rapamycin; p = 0.0002, vehicle versus RapaLink-1; log rank analysis; n = 7 mice per group.

affinity of rapamycin for FKBP12 leads to accumulation of rapamycin in cells (Choi et al., 1996), resulting in durable blockade of p-RPS6^{S235/236}. Having observed increased in vivo potency of RapaLink-1 compared with both rapamycin and MLN0128, we therefore examined whether the proposed binding of RapaLink-1 to FKBP12 might lead to durable mTORC1 inhibition in human glioma cells. We treated LN229 and U87MG cells with RapaLink-1 for 1 day followed by washout, assessing relative growth and signaling (Figures 5A, 5B, and S4B–S4D). Proliferation was blocked for days, with recovery starting between days 2 and 4 (Figures 5A and S4C). RapaLink-1 inhibited phosphorylation of RPS6 and 4EBP1 in a time-dependent manner, with persistent target inhibition over 24 hr, and some recovery by 48 hr (Figures 5B and S4D). In contrast, recovery of proliferation in cells treated with MLN0128 started after 1 day (Figures 5A and S5C), and recovery of signaling was observed at 1 hr after washout (Figures 5B and S4D). Rapamycin durably blocked p-RPS6^{S235/236} but not p-4EBP1^{T37/46}, with minimal anti-proliferative activity in the GBM lines tested (Figures 5A, 5B, and S4B–S4D).

The immunosuppressive FK-506 does not inhibit mTORC1, but it competes with rapamycin for FKBP12 binding. Since FK-506 can block the effects of rapamycin (Shimobayashi and Hall, 2014), we next assessed how FK-506 or rapamycin affected growth inhibition or signaling changes in response to RapaLink-1 (Figures 5C, 5D, and S4E–S4G). Under conditions of excess FK-506 or rapamycin during the washout, recovery of signaling and proliferation were slightly improved (Figures 5C, 5D, S4F, and S4G). FK-506 by itself had little effect on either signaling or proliferation (Figures 5D and S4E). Consistent with the binding to FKBP12 leading to intracellular accumulation of RapaLink-1 over time, Rapalink-1 treatment of therapy-resistant LN229 and U87MG cells transduced with EGFRvIII (Nagane et al., 1998) decreased steadily over 72 hr (Figure 5E), correlating with a time-dependent decrease in p-RPS6^{S235/236} and p-4EBP1^{T37/46} (Figure 5F). Treatment with RapaLink-1 had no cytotoxic effect (Figure 5G). Thus, rapamycin is a durable inhibitor, but inefficiently blocks p-4EBP1^{T37/46}. MLN0128 efficiently inhibits p-4EBP1^{T37/46}, but shows short residence time. RapaLink-1 both durably and efficiently blocks p-4EBP1^{T37/46}.

FKBP12 Is Required for RapaLink-1 Activity

If RapaLink-1 and rapamycin both require binding to FKBP12 for activity, then rapamycin should be able to block the anti-proliferative activity of RapaLink-1 (Figure 6A). Addition of rapamycin to RapaLink-1 led to a decrease in the anti-proliferative dose response to RapaLink-1 at intermediate doses (Figure 6B), asso-

ciated with increased levels of p-4EBP1^{T37/46} (Figure 6C). In comparison, addition of rapamycin to MLN0128 did not affect the anti-proliferative dose response or levels of p-4EBP1^{T37/46} (Figures 6D and 6E). To test whether FK-506 also competes with RapaLink-1, we treated GBM cells with mTOR inhibitors alone or in combination with FK-506. FK-506 antagonized the inhibitory effects of RapaLink-1 and rapamycin on proliferation and p-RPS6^{S235/236} and p-4EBP1^{T37/46}, but FK-506 did not block the cellular effects of MLN0128 (Figures 6F and 6G). These results suggest that FKBP12 is required for the activity of RapaLink-1.

To directly compare the binding of rapamycin-FKBP12 and RapaLink-1-FKBP12 with mTORC1, we immunoprecipitated mTOR and used western blot analysis for bound FKBP12. Levels of the RapaLink-1-FKBP12 complex bound to mTOR were higher than those of the rapamycin-FKBP12 complex, as shown by increased levels of FKBP12 seen in RapaLink-1-treated cells, compared with rapamycin-treated cells (Figure 6H). The increased affinity of RapaLink-1 for FKBP12 could, in-part, underlie our earlier observations that RapaLink-1 is more effective than rapamycin at suppressing mTORC1 activity and proliferation.

DISCUSSION

Earlier-generation inhibitors of mTOR have limited activity in GBM tumors both preclinically and clinically. It is well-established that rapamycin and other allosteric inhibitors of mTORC1 are potent inhibitors of the mTORC1 target S6K, whereas these agents are relatively inefficient inhibitors of 4EBP1 (reviewed in Barić and Williams, 2014). TORKi have better anti-proliferative properties than allosteric inhibitors. Although improved activity was anticipated based on the ability of orthosteric inhibitors to block mTORC2, the increased efficacy of TORKi was ultimately traced to better inhibition of mTORC1. Specifically, TORKi more effectively block 4EBP1 compared with rapamycin (Feldman et al., 2009; Garcia-Martinez et al., 2009; Thoreen et al., 2009).

As expected, our in vitro studies showed that the clinical TORKi MLN0128 was more effective than rapamycin in cell culture, correlating with improved inhibition of the mTORC1 target 4EBP1. Despite this increased activity; however, we show here that MLN0128 shows a short residence time (Bradshaw et al., 2015) and decreased in vivo activity compared with rapamycin. In addition, despite its inability to block 4EBP1 phosphorylation in vitro, rapamycin did show some blockade of this target in vivo. The improved in vivo efficacy of RapaLink-1 compared with earlier-generation inhibitors of mTOR is likely due both to its

(F) Three animals from each group treated as in (E) were euthanized on day 14. Samples analyzed by immunohistochemistry for Ki67, and the percentage of positive cells was calculated. Data shown are mean \pm SD of five microscopic fields from three tumors in each group. n.s., not significant; p = 0.0503, vehicle versus MLN0128; **p = 0.0023, vehicle versus rapamycin; ***p < 0.0001, vehicle versus RapaLink-1 (two-tailed Student's t test).

(G) Representative images of H&E staining and immunohistochemistry for Ki-67 from tumors in (F). Scale bars, 100 μ m.

(H) GTML mice with luciferase activity of 10^7 photons/s were randomized into two groups and treated by i.p. injections of vehicle (daily) or RapaLink-1 (1.5 mg/kg, every 5 days). Bioluminescence imaging was obtained at 0, 5, 11, 15, 20, 25, 29, and 35 days after starting treatment using identical imaging conditions.

(I) Regions of interest from displayed images in (H) were revealed on the tumor sites and quantified as maximum photons/s/cm²/steradian. Data shown are mean \pm SD (vehicle n = 4; RapaLink-1 n = 3). *p = 0.0373 by two-tailed Student's t test.

(J) Two GTML mice from each group with luciferase activity of 10^8 photons/s were treated as in (H) at day 5 after starting treatment were injected with vehicle or RapaLink-1 (1.5 mg/kg) 30 min prior to being euthanized, and tumors were harvested, lysed, and analyzed by western blotting as indicated.

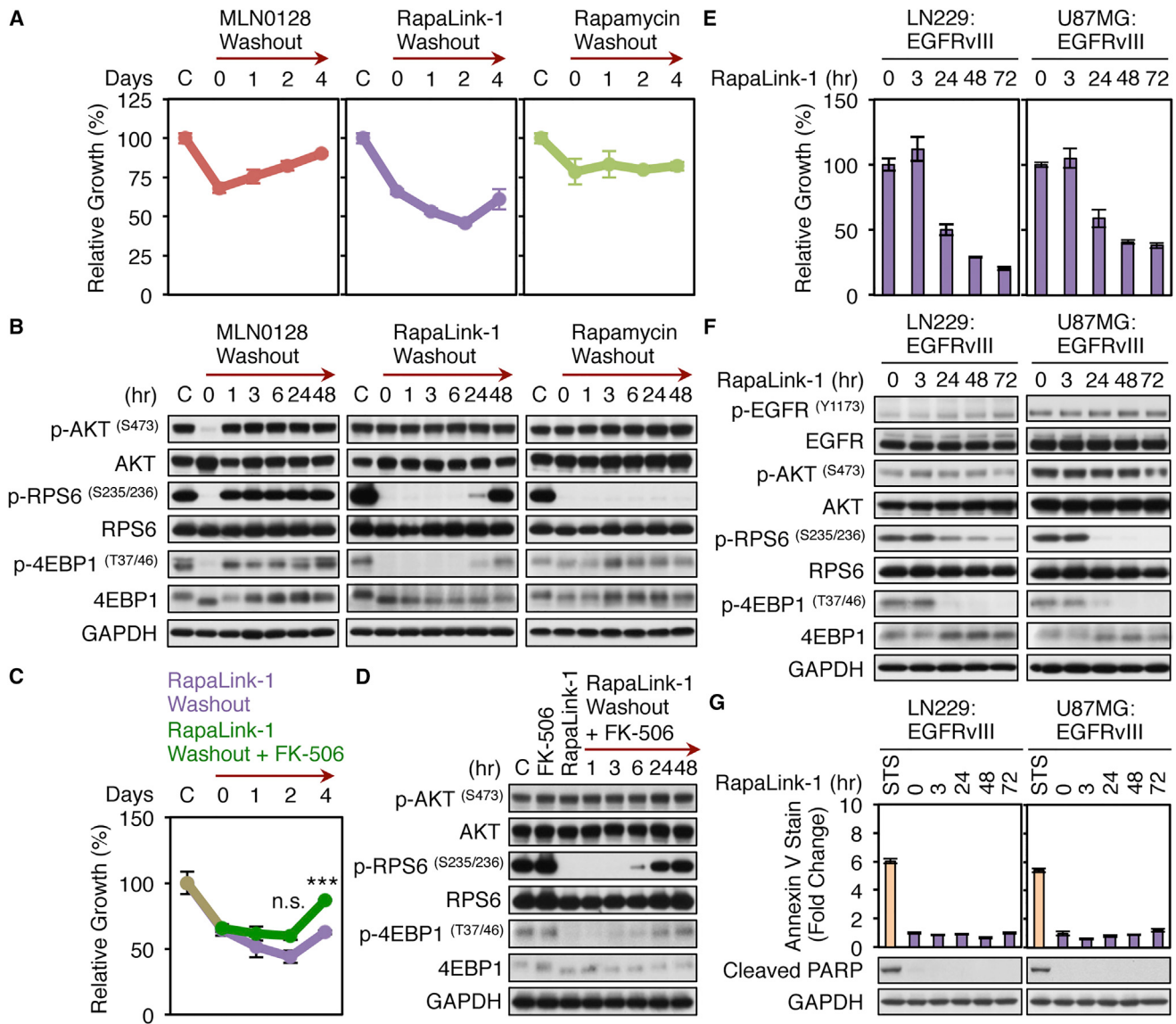


Figure 5. RapaLink-1 Accumulates in Cells, Durably Blocking mTORC1

(A) U87MG cells were treated with 200 nM MLN0128, 1.56 nM RapaLink-1, or 10 nM rapamycin for 24 hr. Cells were resuspended in medium without inhibitors and grown for the amounts of time indicated (0–4 days). Proliferation was measured by WST-1 assay. Data shown are mean \pm SD (percentage growth relative to DMSO-treated control) of triplicate measurements.

(B) Cells were treated as in (A) for 24 hr. Cells were resuspended in medium without inhibitors, grown for times indicated (1–48 hr), harvested, lysed, and analyzed by western blotting as indicated. Representative blots from three independent experiments are shown.

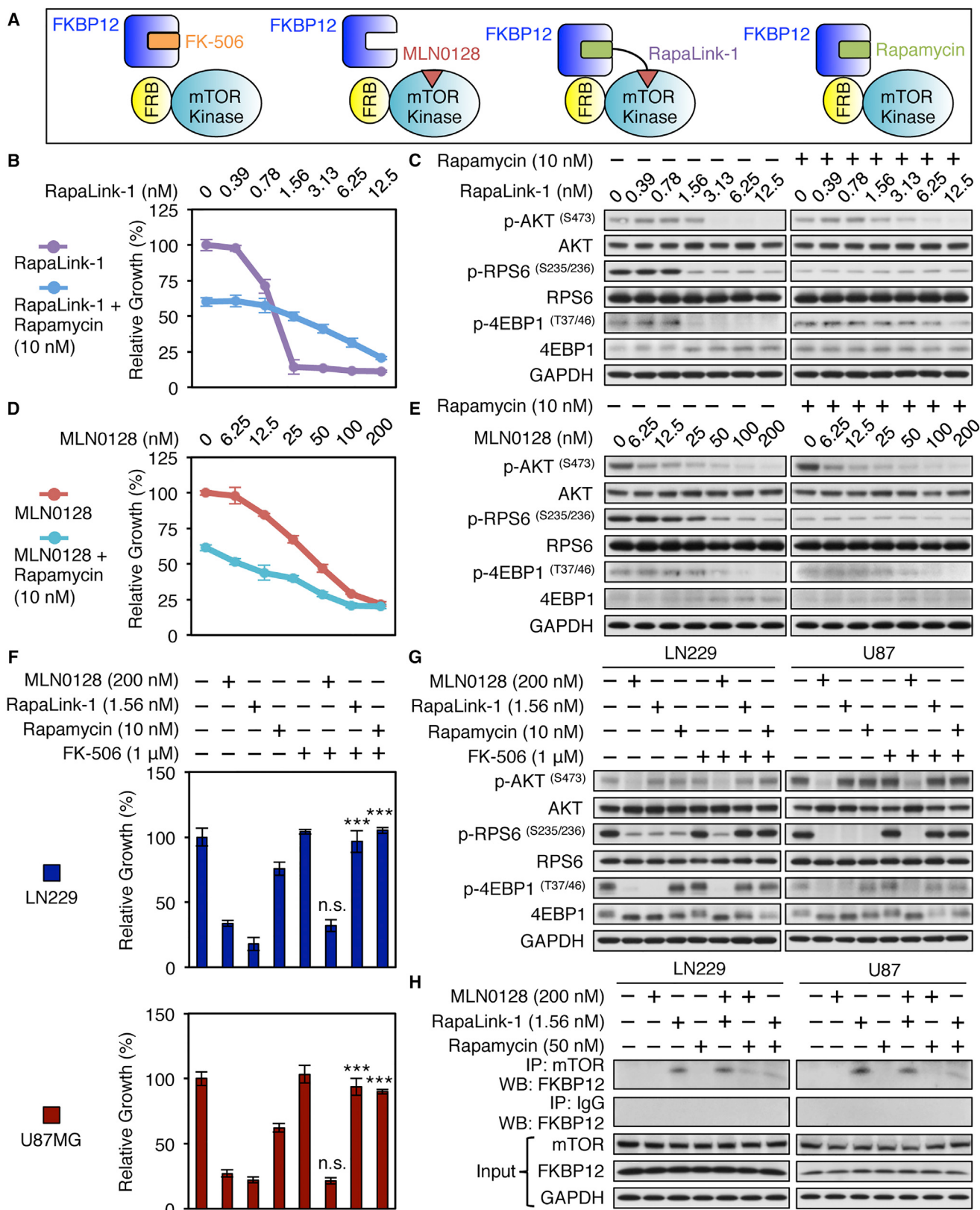
(C) U87MG cells were treated with DMSO or 1.56 nM RapaLink-1 for 24 hr (left two lanes). Cells treated with RapaLink-1 for 24 hr were resuspended in medium with or without 1 μ M FK-506 in the absence of RapaLink-1 for 1–4 days (right three lanes). Proliferation was measured by WST-1 assay. n.s., not significant; day 2, RapaLink-1 washout versus RapaLink-1 washout + FK-506, $p = 0.08$; day 4, RapaLink-1 washout versus RapaLink-1 washout + FK-506, *** $p < 0.0001$. Data shown represent mean \pm SD (percentage growth relative to DMSO-treated control) of triplicate measurements. The C group represents DMSO treatment alone.

(D) U87MG cells were treated with DMSO, 1 μ M FK-506, or 1.56 nM RapaLink-1 for 24 hr (left three lanes). Cells treated with RapaLink-1 for 24 hr were resuspended in medium with 1 μ M FK-506 in the absence of RapaLink-1, and grown for 1–48 hr (right 5 lanes). Cells were harvested, lysed, and analyzed by western blotting as indicated. Representative blots from two independent experiments are shown. The C group represents DMSO treatment alone.

(E) LN229:EGFRvIII and U87MG:EGFRvIII cells were treated with 1.56 nM RapaLink-1 for the times indicated. Proliferation was measured by WST-1 assay. Data shown are mean \pm SD (percentage growth relative to DMSO-treated control) of triplicate measurements.

(F) Cells treated as in (E) were harvested, lysed, and analyzed by western blotting as indicated.

(G) Apoptotic cells treated as in (E) were analyzed by flow cytometry for Annexin V. Cells treated with 1 μ M staurosporine (STS) for 24 hr were used as a positive control. Data shown represent mean \pm SD (fold change compared with RapaLink-1 0 hr treatment) of triplicate measurements. An aliquot of cells was analyzed by western blotting as indicated (bottom panel). See also Figure S4.



(legend on next page)

ability to efficiently block 4EBP1 (compared with rapamycin and MLN0128) and its prolonged residence time (compared with MLN0128).

Levels of FKBP12 bound to mTOR were higher in cells treated with RapaLink-1 compared with cells treated with rapamycin. The rapamycin-FKBP12 complex binds only to FRB, whereas the RapaLink-1-FKBP12 complex can bind both to FRB and to the mTORC1 kinase domain. This dual binding may serve to increase affinity and stability, both of which likely contribute to efficacy. Despite its size, RapaLink-1 crossed the blood-brain barrier and could induce regression in orthotopic xenograft, PDX, and genetically engineered models for brain cancer. This class of agents thus holds promise for future therapy of patients with GBM.

While RapaLink-1 promoted regression in GBM models, this initial regression was followed by regrowth of the tumor. Such recurrence is consistent with data suggesting that mTOR inhibitors as monotherapies are not sufficient to achieve anti-tumor responses in most cancers (Ilagan and Manning, 2016). Studies to establish the basis for recurrence, such as induction of autophagy, feedback loops, rewiring, or other modes of acquired resistance, and to identify combinations that promote apoptosis and that block emergent resistance would help to position RapaLink-1 for clinical development.

EXPERIMENTAL PROCEDURES

Cell Lines, Reagents, Transfection, and Transduction

Human glioma cell lines were grown in 10% fetal bovine serum. These included LN229, U87MG, GBM43, GBM5, and GBM12 (Sarkaria et al., 2006). Plasmids pcDNA3-mTOR^{WT}, pcDNA3-mTOR^{R2505P}, pcDNA3-mTOR^{S2215Y} (Sato et al., 2010) were obtained from Addgene (plasmid nos. 26036–8); and transfected stably into LN229 cells using Effectene Transfection Reagent (QIAGEN). To generate retrovirus to transduce LN229 and U87MG with EGFR or EGFRvIII (Fan et al., 2007), the packaging cell line 293T was co-transfected with pWLZ-hygro-EGFR plasmid gag/pol and VSVg or with pLRNL-neo-EGFRvIII plasmid gag/pol and VSVg again using Effectene. High-titer virus was collected at 48 hr and used to infect cells as described (Fan et al., 2006). Transfected and transduced cells were selected as pools with G418 (800 µg/mL) or hygromycin (500 µg/mL) for 2 weeks. Inhibitors INK1437, TGX221, IC87114, INK1358, AS252424, AS605240, and GDC-0941 were from Pingda Ren and

Liansheng Li. AKT inhibitor VIII was from EMD Biosciences. Rapamycin was from Cell Signaling Technology. NVP-BEZ235, MLN0128, and MK-2206 were from Selleck Chemicals. KU-0063794 and FK-506 were from Sigma-Aldrich Inc. Insulin was from Eli Lilly. D-Luciferin was from Gold Biotechnology. RapaLink-1 and RapaLink-2 were synthesized by C.M., M.O., and K.M.S. as described previously (Rodrik-Outmezguine et al., 2016).

Cell Proliferation Assays, Apoptosis Detection, and Flow Cytometry

For proliferation, 5×10^4 cells were seeded in 12-well plates and treated as indicated for 3 days. Proliferation was determined by WST-1 absorbance (Roche), read at 40 min. For flow cytometry, 5×10^5 cells were seeded in six-well plates and treated as indicated for 24 hr. Cells were harvested and fixed in 70% ethanol for 30 min, stained with 5 µg/mL propidium iodide containing 125 unit/mL RNase, and filtered through a 35 µm nylon mesh (Corning Life Sciences). Ten thousand stained nuclei were analyzed in a FACSCalibur flow cytometer (Becton Dickinson). DNA histograms were modeled offline using ModFit-LT software (Verity Software House). Apoptosis was detected by measurement of SubG1 fraction, by western blotting for cleaved poly(ADP-ribose) polymerase, or by flow cytometry for Annexin V-FITC as per the manufacturer's protocol (Annexin V-FITC Detection Kit, BioVision Technologies) using FlowJo software (Tree Star).

PIP3/PI(4,5)P2 Quantification

PIP3/PI(4,5)P2 levels were measured by ELISA (Echelon K-2500s). In brief, 10^7 cells were seeded in 10 cm plates, treated as indicated for 3 hr, harvested with cold 0.5 M tricarboxylic acid, and centrifuged. Pellets were suspended in 5% tricarboxylic acid/1 µM EDTA, vortexed, and centrifuged. Neutral lipids were extracted in MeOH:CHCl₃ (2:1), vortexed, and centrifuged. Acidic lipids were extracted by adding 2.25 mL MeOH:CHCl₃:12 N HCl (80:40:1), vortexed, and centrifuged. CHCl₃ (0.75 mL) and 0.1 M HCl (1.35 mL) were added to the supernatant. Samples were vortexed, and centrifuged, collecting the lower organic phase. Samples were dried, resuspended in 200 µL of PBS-Tween 3% protein stabilizer, and sonicated before adding to the ELISA. Each sample was assayed in triplicate and absorbance (450 nm) read on a plate reader.

Western Blotting

Membranes were blotted with p-AKT^{T308}, p-AKT^{S473}, AKT, p-NDRG1^{T346}, NDRG1, p-SGK1^{S78}, SGK1, p-GSK3β^{S9}, GSK3β, p-S6 ribosomal protein^{S235/S236}, S6 ribosomal protein, p-4EBP1^{T37/T46}, and 4EBP1 (Cell Signaling Technology), p-EGFR^{Y1173}, FKBP12 (Novus Biologicals), EGFR, mTOR, normal mouse immunoglobulin G (IgG) (Santa Cruz Biotechnology), GAPDH, or β-tubulin (Upstate Biotechnology). Bound antibodies were detected with horseradish peroxidase-linked anti-mouse or anti-rabbit IgG (Calbiochem), followed by ECL (Amersham).

Figure 6. FKBP12 Is Required for RapaLink-1 and Rapamycin Activity

- (A) Model: FKBP12 bound to rapamycin or RapaLink-1 can interact with the FRB domain of mTORC1, whereas FKBP12 binding is not required for MLN0128.
- (B) LN229 cells were treated with RapaLink-1 alone or in combination with rapamycin at the doses indicated. Proliferation was measured by WST-1 assay after treatment for 3 days. Data shown represent mean ± SD (percentage growth relative to DMSO-treated control) of triplicate measurements.
- (C) Cells treated as in (B) for 3 hr were harvested, lysed, and analyzed by western blotting as indicated. Cell lysates were from a single experiment. Gels were run for the same period of time, and blots were processed with equivalent exposure times, to assure reproducibility. Representative blots from two independent experiments are shown.
- (D) LN229 cells were treated with MLN0128 alone or with rapamycin at the doses indicated. Proliferation was measured by WST-1 assay after treatment for 3 days. Data shown are mean ± SD (percentage growth relative to DMSO-treated control) of triplicate measurements.
- (E) Cells treated as in (D) for 3 hr were harvested, lysed, and analyzed by western blotting using antisera indicated. Cell lysates were from a single experiment. Gels were run for the same period of time, and blots were processed with equivalent exposure times, to assure reproducibility. Representative blots from two independent experiments are shown.
- (F) LN229 and U87MG cells were pre-treated with FK-506 for 30 min and then treated with mTOR inhibitors alone or with FK-506 at doses indicated for 3 days. Cell proliferation was measured by WST-1 assay. Data shown are mean ± SD (percentage growth relative to DMSO-treated control) of triplicate measurements. n.s., not significant MLN0128 versus MLN0128 + FK-506; ***p < 0.001 RapaLink-1 versus RapaLink-1 + FK-506; **p < 0.001 rapamycin versus rapamycin + FK-506 by two-tailed Student's t test.
- (G) Cells treated as in (F) for 3 hr were harvested, lysed, and analyzed by western blotting as indicated. Representative blots from two independent experiments are shown.
- (H) LN229 and U87MG cells were treated with inhibitors as indicated for 24 hr. mTOR was immunoprecipitated using a mouse monoclonal mTOR antibody, and immunoprecipitates (IP) were analyzed by western blotting (WB) to detect FKBP12. Mouse IgG was used as negative control. Whole-cell lysates blotted with mTOR, FKBP12, and GAPDH antibodies served as input controls. Representative blots from three independent experiments are shown.

Immunoprecipitation

Protein (200 µg) was incubated with 1 µg anti-mTOR mouse monoclonal antibody (Santa Cruz Biotechnology) or control mouse IgG at 4°C overnight with gentle agitation. Protein G agarose (40 µL) was added, and samples incubated for 1 hr at 4°C. Immunocomplexes were then pelleted, washed multiple times at 4°C, and subjected to SDS-PAGE and western blotting, using anti-FKBP12 rabbit polyclonal antibody (Cell Signaling Technology).

In Vitro Luciferase Assay and Bioluminescence Imaging

Luciferase-modified GBM43 and GBM5 cells (1×10^5) were plated on 24-well plates and treated with MLN0128, RapaLink-1, or rapamycin for 3 days. D-Luciferin was added to a final concentration of 0.6 mg/mL. After 10 min, luminescence was measured on an IVIS Lumina System (Caliper Life Science) with Living Image software. Mice were injected i.p. with 64 mg/kg (U87MG and GBM43) or with 80 mg/kg (GTML) of D-luciferin dissolved in sterile saline. Tumor bioluminescence was determined 20 min after D-luciferin injection, as the sum of photon counts/s in regions of interest, defined by a lower threshold value of 25% of peak pixel intensity. Imaging was performed every 5 days after tumor implantation until the last day on which all mice in all groups were alive.

Immunohistochemical Analyses

Immunohistochemical stains were performed by the UCSF Brain Tumor Research Center Tissue Core. After resection, mouse brains (three per group) were fixed for 12 hr in 4% paraformaldehyde in PBS. Brains were paraffin-embedded, and sectioned (5 µm) for H&E staining and immunohistochemical analyses. Immunostaining was performed using a Benchmark XT automated stainer (Ventana Medical Systems). Sections were immunostained with antibodies against Ki67 (mouse monoclonal DAK-H1-WT, Dako, diluted 1:100). Antibodies were detected with the Ventana iVIEW DAB Detection Kit (yielding a brown reaction product). Slides were counterstained with hematoxylin, dehydrated and mounted in DePeX mounting medium (SERVA).

Complete Blood Count and Chemistry Panel Testing

BALB/C^{nu/nu} mice (three mice each group, Simonsen Laboratories) were treated on day 0 with i.p. injections of vehicle (daily), MLN0128 (1.5 mg/kg, daily), rapamycin (1.5 mg/kg, daily), or RapaLink-1 (1.5 mg/kg, every 5 days) and euthanized on days 1, 3, and 7. Blood samples were collected by cardiac puncture under anesthesia. Blood was collected into EDTA anti-coagulant tubes. Blood counts were measured using a Bio-Rad TC20 automated cell counter. For serum collection, blood was allowed to clot for at least 30 min at room temperature before serum separation by centrifugation at 3,000 × g for 15 min. Levels of alanine transaminase, aspartate transaminase, and blood urea nitrogen were measured by IDEXX Laboratories.

In Vivo Studies

All animal experiments were conducted using protocols approved by University of California, San Francisco's Institutional Animal Care and Use Committee (IACUC). GTML mouse models were described previously (Swartling et al., 2010). Three 4- to 6-week-old female athymic BALB/C^{nu/nu}, per group were treated with i.p. injections of vehicle (20% DMSO, 40% PEG-300, and 40% PBS [v/v]), MLN0128 (16 mg/kg), RapaLink-1 (0.4 mg/kg), RapaLink-1 (4 mg/kg), or rapamycin (4 mg/kg) for 15 min, followed by i.p. injection of 250 mU insulin or saline, then killed 15 min later. Skeletal muscle, liver, and brain of each mouse were lysed, and analyzed by western blotting. Orthotopic injections and treatment studies: female BALB/C^{nu/nu}, mice (4 to 6 weeks old) were anesthetized using ketamine and xylazine. U87MG (3×10^5) or GBM43 cells (1×10^5) expressing firefly luciferase were injected intracranially (Hamilton syringe) at coordinates 2 mm anterior and 1.5 mm lateral of the right hemisphere relative to bregma, at a depth of 3 mm. Whole-brain bioluminescence was measured for each mouse every 3 to 5 days. When bioluminescence reached 10^5 photons/s (GBM43) or 10^7 photons/s (U87MG), mice were sorted into four groups of equal mean bioluminescent signal (10 to 12 mice per group), and therapy initiated. For U87MG orthotopic xenografts, groups were treated with i.p. injection of vehicle (20% DMSO, 40% PEG-300, and 40% PBS [v/v], daily), MLN0128 (1.5 mg/kg daily), rapamycin (1.5 mg/kg), or RapaLink-1 (1.5 mg/kg every 5 days for 25 days, then once a week for 6 weeks). For GBM43 patient-derived xenografts, mice were treated with i.p. injection of vehicle (13.3% Cremophor-EL, 6.7% EtOH in 0.9% NaCl, daily), MLN0128

(1.5 mg/kg daily), rapamycin (5 mg/kg), or RapaLink-1 (1.5 mg/kg every 5 days). Sucrose was supplemented to 15% in drinking water. Mice were monitored daily and euthanized when they exhibited neurological deficits or 15% reduction from initial body weight. Preparation of vehicle and RapaLink-1, sucrose supplementation, and dosing schedule for GTML mice were identical to that described in GBM43 experiments.

Statistical Analysis

Survival analysis was performed using the GraphPad Prism 6 program (GraphPad), significance was determined by the log rank (Mantel-Cox) test. For all other analyses, a two-tailed unpaired Student's t test was applied.

SUPPLEMENTAL INFORMATION

Supplemental Information includes four figures and can be found with this article online at <http://dx.doi.org/10.1016/j.ccr.2017.01.014>.

AUTHOR CONTRIBUTIONS

Q.W.F., K.M.S., and W.A.W. conceived the project. Q.W.F., R.A.W., S.I., and A.Y.Q.T. performed in vitro experiments and in vivo experiments with the U87MG model. A.Y.Q.T. and T.N. performed in vitro experiments, and Q.W.F., G.C., and E.F.S. performed in vivo experiments with the GBM43 model. O.A. performed in vivo experiments with the GTML model. J.J.P. analyzed immunohistochemistry. C.J.N. and M.O. provided RapaLink-1. C.J.N., M.O., W.C.G., and D.H.K. analyzed data. Q.W.F. and W.A.W. wrote the manuscript.

ACKNOWLEDGMENTS

We thank Francis Burrows, Arman Jahangiri, and Yi Liu for critical review, Pingda Ren and Liansheng Li for small-molecule inhibitors, and David James for GBM5, GBM12, and GBM43. K.M.S. is an inventor on patents related to MLN0128 held by the University of California, San Francisco, and sublicensed to Takeda Pharmaceuticals. M.O. is an employee of, and K.M.S. is a consultant to Takeda Pharmaceutical Company, Limited, which is conducting MLN0128 clinical trials. Supported by NIH grants R01NS091620, R01NS089868, R01CA148699, R01NS089868, U01CA176287, P30CA82103, U54CA163155, P50AA017072, and Kura Oncology; as well as Children's Tumor, CureSearch, Ross K. MacNeill, and the Samuel Waxman Cancer Research Foundations.

Received: January 26, 2016

Revised: August 19, 2016

Accepted: January 26, 2017

Published: March 13, 2017

REFERENCES

- Barić, D., and Williams, R.L. (2014). The structural basis for mTOR function. *Semin. Cell Dev. Biol.* 36, 91–101.
- Bradshaw, J.M., McFarland, J.M., Paavilainen, V.O., Bisconte, A., Tam, D., Phan, V.T., Romanov, S., Finkle, D., Shu, J., Patel, V., et al. (2015). Prolonged and tunable residence time using reversible covalent kinase inhibitors. *Nat. Chem. Biol.* 11, 525–531.
- Brennan, C.W., Verhaak, R.G.W., McKenna, A., Campos, B., Noushmehr, H., Salama, S.R., Zheng, S., Chakravarty, D., Sanborn, J.Z., Berman, S.H., et al. (2013). The somatic genomic landscape of glioblastoma. *Cell* 155, 462–477.
- Chiu, M.I., Katz, H., and Berlin, V. (1994). RAPT1, a mammalian homolog of yeast Tor, interacts with the FKBP12/rapamycin complex. *Proc. Natl. Acad. Sci. USA* 91, 12574–12578.
- Choi, J., Chen, J., Schreiber, S.L., and Clardy, J. (1996). Structure of the FKBP12-rapamycin complex interacting with the binding domain of human FRAP. *Science* 273, 239–242.
- Fan, Q.-W., Knight, Z.A., Goldenberg, D.D., Yu, W., Mostov, K.E., Stokoe, D., Shokat, K.M., and Weiss, W.A. (2006). A dual PI3 kinase/mTOR inhibitor reveals emergent efficacy in glioma. *Cancer Cell* 9, 341–349.

- Fan, Q.-W., Cheng, C.K., Nicolaides, T.P., Hackett, C.S., Knight, Z.A., Shokat, K.M., and Weiss, W.A. (2007). A dual phosphoinositide-3-kinase [α]/mTOR inhibitor cooperates with blockade of epidermal growth factor receptor in PTEN-mutant glioma. *Cancer Res.* 67, 7960–7965.
- Fan, Q.-W., Cheng, C., Knight, Z.A., Haas-Kogan, D., Stokoe, D., James, C.D., McCormick, F., Shokat, K.M., and Weiss, W.A. (2009). EGFR signals to mTOR through PKC and independently of Akt in glioma. *Sci. Signal* 2, ra4.
- Feldman, M.E., Apsel, B., Uotila, A., Loewith, R., Knight, Z.A., Ruggero, D., and Shokat, K.M. (2009). Active-site inhibitors of mTOR target rapamycin-resistant outputs of mTORC1 and mTORC2. *PLoS Biol.* 7, e38.
- Folkes, A.J., Ahmadi, K., Alderton, W.K., Alix, S., Baker, S.J., Box, G., Chuckowree, I.S., Clarke, P.A., Depledge, P., Eccles, S.A., et al. (2008). The identification of 2-(1H-indazol-4-yl)-6-(4-methanesulfonyl-piperazin-1-ylmethyl)-4-morpholin-4-yl-thieno[3,2-d]pyrimidine (GDC-0941) as a potent, selective, orally bioavailable inhibitor of class I PI3 kinase for the treatment of cancer. *J. Med. Chem.* 51, 5522–5532.
- Garcia-Martinez, J.M., Moran, J., Clarke, R.G., Gray, A., Cosulich, S.C., Chresta, C.M., and Alessi, D.R. (2009). Ku-0063794 is a specific inhibitor of the mammalian target of rapamycin (mTOR). *Biochem. J.* 421, 29–42.
- Gaubitz, C., Oliveira, T.M., Prouteau, M., Leitner, A., Karuppasamy, M., Konstantinidou, G., Rispal, D., Eltschinger, S., Robinson, G.C., Thore, S., et al. (2015). Molecular basis of the rapamycin insensitivity of target of rapamycin complex 2. *Mol. Cell* 58, 977–988.
- Hirai, H., Sootome, H., Nakatsuru, Y., Miyama, K., Taguchi, S., Tsujioka, K., Ueno, Y., Hatch, H., Majumder, P.K., Pan, B.-S., et al. (2010). MK-2206, an allosteric Akt inhibitor, enhances antitumor efficacy by standard chemotherapeutic agents or molecular targeted drugs *in vitro* and *in vivo*. *Mol. Cancer Ther.* 9, 1956–1967.
- Houghton, P.J., Morton, C.L., Gorlick, R., Lock, R.B., Carol, H., Reynolds, C.P., Kang, M.H., Maris, J.M., Keir, S.T., Kolb, E.A., et al. (2010). Stage 2 combination testing of rapamycin with cytotoxic agents by the Pediatric Preclinical Testing Program. *Mol. Cancer Ther.* 9, 101–112.
- Hsieh, A.C., Liu, Y., Edlind, M.P., Ingolia, N.T., Janes, M.R., Sher, A., Shi, E.Y., Stumpf, C.R., Christensen, C., Bonham, M.J., et al. (2012). The translational landscape of mTOR signalling steers cancer initiation and metastasis. *Nature* 485, 55–61.
- Ilagan, E., and Manning, B.D. (2016). Emerging role of mTOR in the response to cancer therapeutics. *Trends Cancer* 2, 241–251.
- Loewith, R., Jacinto, E., Wullschleger, S., Lorberg, A., Crespo, J.L., Bonenfant, D., Oppiger, W., Jenoe, P., and Hall, M.N. (2002). Two TOR complexes, only one of which is rapamycin sensitive, have distinct roles in cell growth control. *Mol. Cell* 10, 457–468.
- MacMillan, D. (2013). FK506 binding proteins: cellular regulators of intracellular Ca²⁺ signalling. *Eur. J. Pharmacol.* 700, 181–193.
- Nagane, M., Levitzki, A., Gazit, A., Cavenee, W.K., and Huang, H.J. (1998). Drug resistance of human glioblastoma cells conferred by a tumor-specific mutant epidermal growth factor receptor through modulation of Bcl-XL and caspase-3-like proteases. *Proc. Natl. Acad. Sci. USA* 95, 5724–5729.
- Omuro, A., and DeAngelis, L.M. (2013). Glioblastoma and other malignant gliomas: a clinical review. *JAMA* 310, 1842–1850.
- Rodrik-Outmezguine, V.S., Okaniwa, M., Yao, Z., Novotny, C.J., McWhirter, C., Banaji, A., Won, H., Wong, W., Berger, M., De Stanchina, E., et al. (2016). Overcoming mTOR resistance mutations with a new-generation mTOR inhibitor. *Nature* 534, 272–276.
- Sarkaria, J.N., Carlson, B.L., Schroeder, M.A., Grogan, P., Brown, P.D., Giannini, C., Ballman, K.V., Kitange, G.J., Guha, A., Pandita, A., et al. (2006). Use of an orthotopic xenograft model for assessing the effect of epidermal growth factor receptor amplification on glioblastoma radiation response. *Clin. Cancer Res.* 12, 2264–2271.
- Sato, T., Nakashima, A., Guo, L., Coffman, K., and Tamanoi, F. (2010). Single amino-acid changes that confer constitutive activation of mTOR are discovered in human cancer. *Oncogene* 29, 2746–2752.
- Shimobayashi, M., and Hall, M.N. (2014). Making new contacts: the mTOR network in metabolism and signalling crosstalk. *Nat. Rev. Mol. Cell Biol.* 15, 155–162.
- Sun, S.Y., Rosenberg, L.M., Wang, X., Zhou, Z., Yue, P., Fu, H., and Khuri, F.R. (2005). Activation of Akt and eIF4E survival pathways by rapamycin-mediated mammalian target of rapamycin inhibition. *Cancer Res.* 65, 7052–7058.
- Swartling, F.J., Grimmer, M.R., Hackett, C.S., Northcott, P.A., Fan, Q.-W., Goldenberg, D.D., Lau, J., Masic, S., Nguyen, K., Yakovenko, S., et al. (2010). Pleiotropic role for MYCN in medulloblastoma. *Genes Dev.* 24, 1059–1072.
- Taylor, T.E., Furnari, F.B., and Cavenee, W.K. (2012). Targeting EGFR for treatment of glioblastoma: molecular basis to overcome resistance. *Curr. Cancer Drug Targets* 12, 197–209.
- Thoreen, C.C., Kang, S.A., Chang, J.W., Liu, Q., Zhang, J., Gao, Y., Reichling, L.J., Sim, T., Sabatini, D.M., and Gray, N.S. (2009). An ATP-competitive mTOR inhibitor reveals rapamycin-insensitive functions of mTORC1. *J. Biol. Chem.* 284, 8023–8032.